

Supplement of Atmos. Chem. Phys., 19, 4419–4437, 2019
<https://doi.org/10.5194/acp-19-4419-2019-supplement>
© Author(s) 2019. This work is distributed under
the Creative Commons Attribution 4.0 License.



Supplement of

Solubility and solution-phase chemistry of isocyanic acid, methyl isocyanate, and cyanogen halides

James M. Roberts and Yong Liu

Correspondence to: James M. Roberts (james.m.roberts@noaa.gov)

The copyright of individual parts of the supplement might differ from the CC BY 4.0 License.

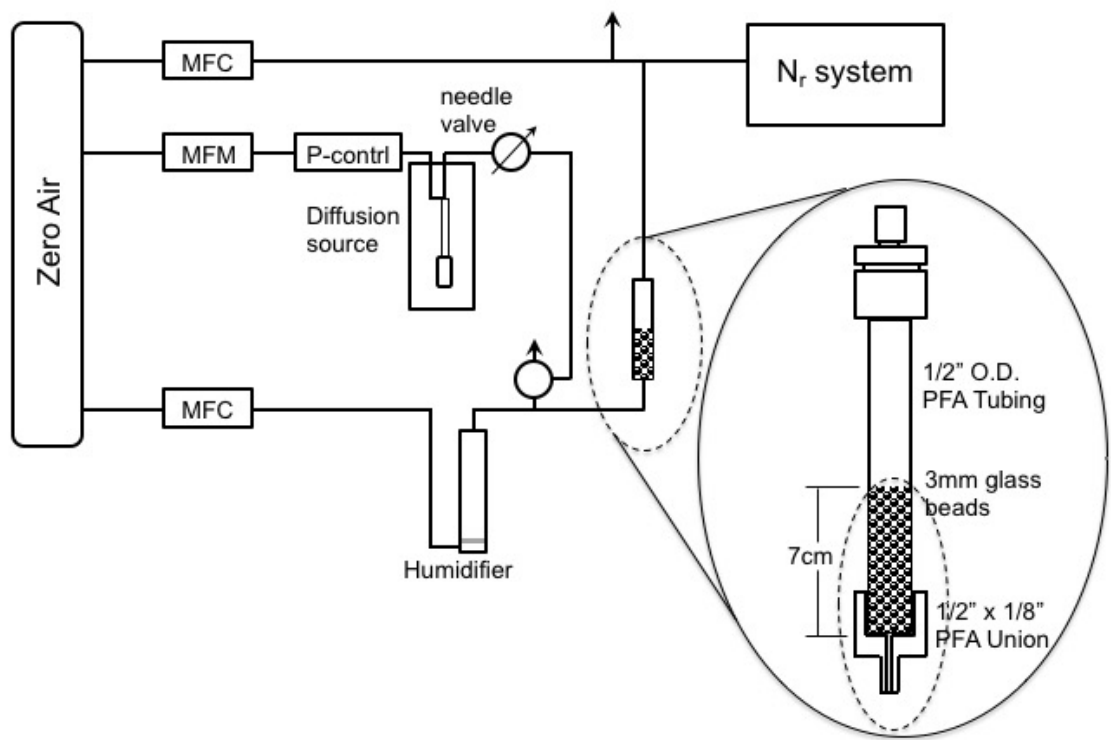


Figure S1., The small-scale Teflon PFA reactor used for ICN solubility measurements.

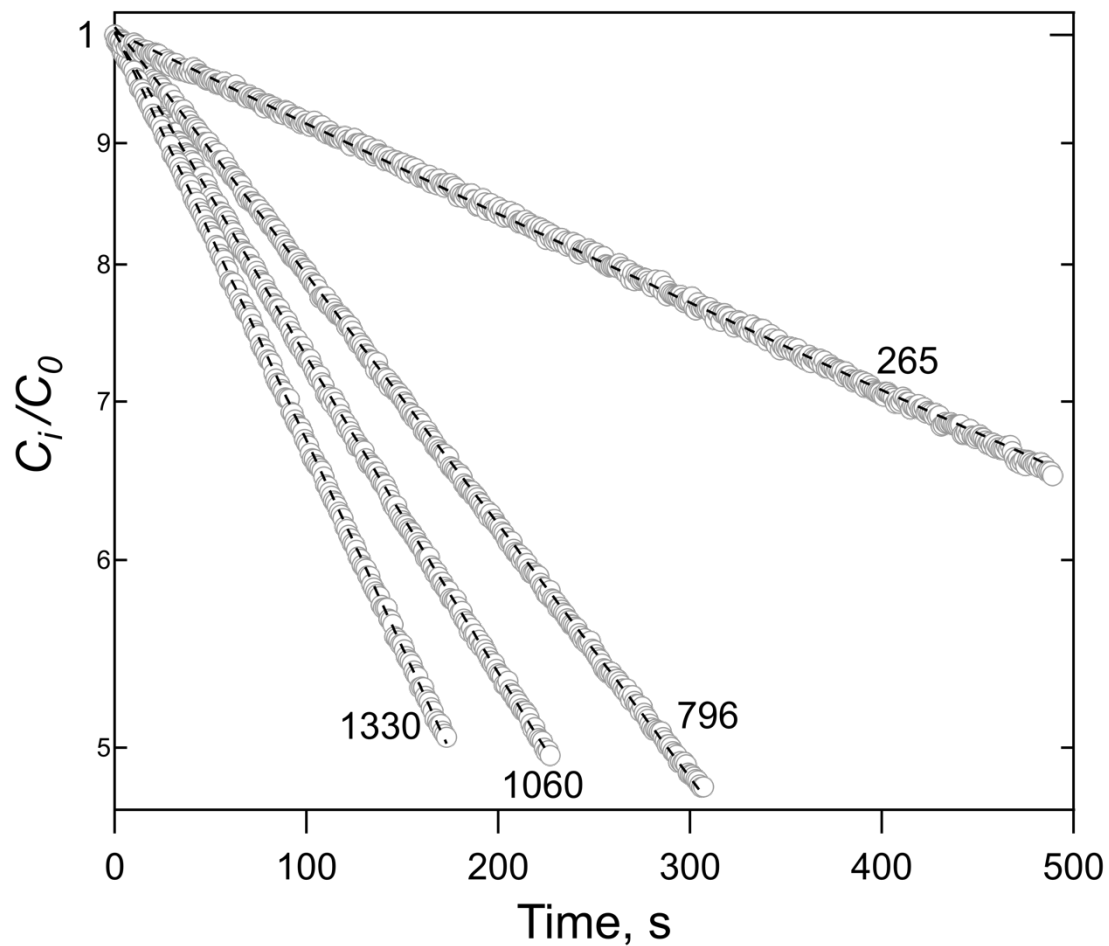


Figure S2. The decay curves corresponding to the measurement of HNCO solubility in 21.9 cc of 10% n-octanol in tridecane at 299K, for which the results are shown in Figure 2 of the main paper. The dashed lines are exponential fits and the numbers shown are the flow rates in amb cc/min.

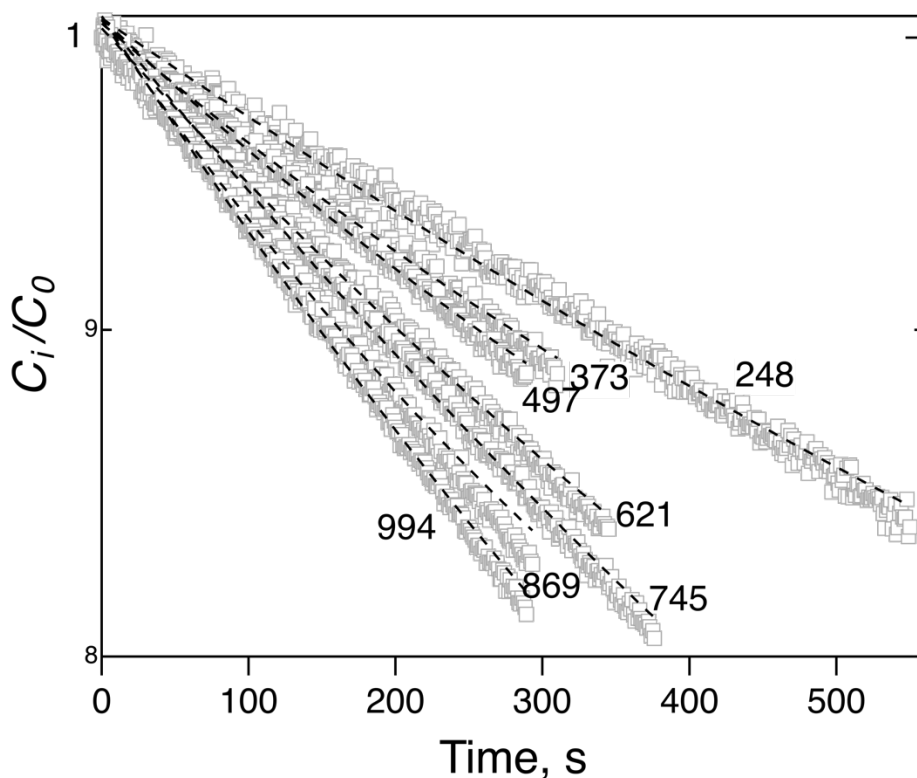


Figure S3. The decay curves corresponding to the measurement of H₂CO solubility in 20 cc of H₂O at pH3 and 279K. The dashed lines are exponential fits and the numbers shown are the flow rates in amb cc/min.

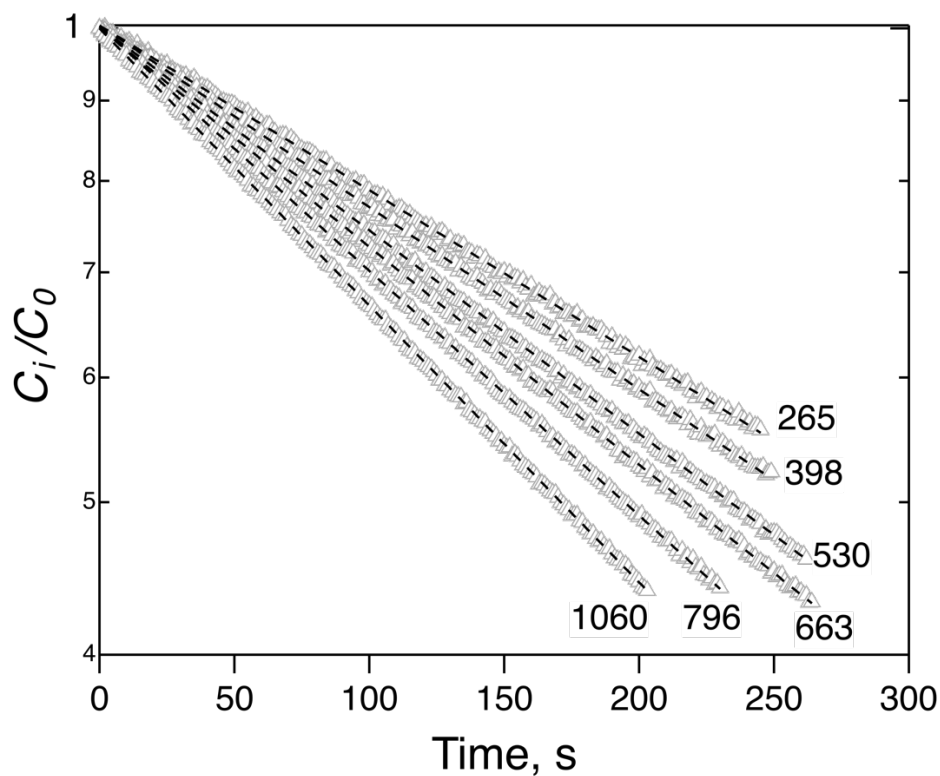


Figure S4. The decay curves corresponding to the measurement of H₂CO solubility in 20 cc of H₂O at pH2 and 298K. The dashed lines are exponential fits and the numbers shown are the flow rates in amb cc/min.

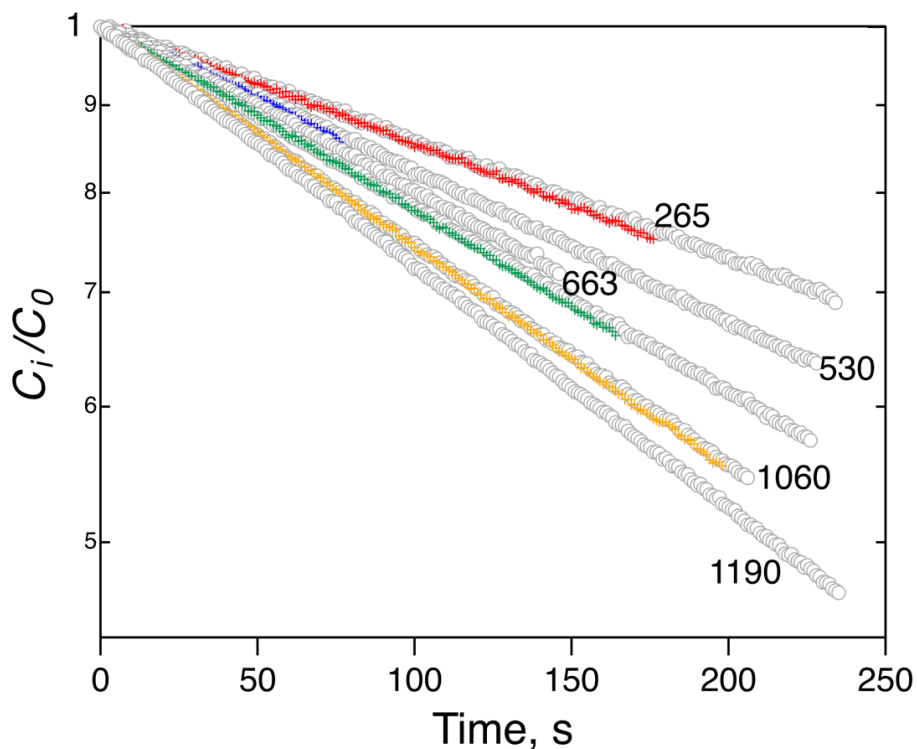


Figure S5. The decay curves corresponding to the measurement of HNCO solubility in 20 cc of H₂O at 1M NaCl, pH3 and 298K. The numbers shown are the flow rates in amb cc/min.

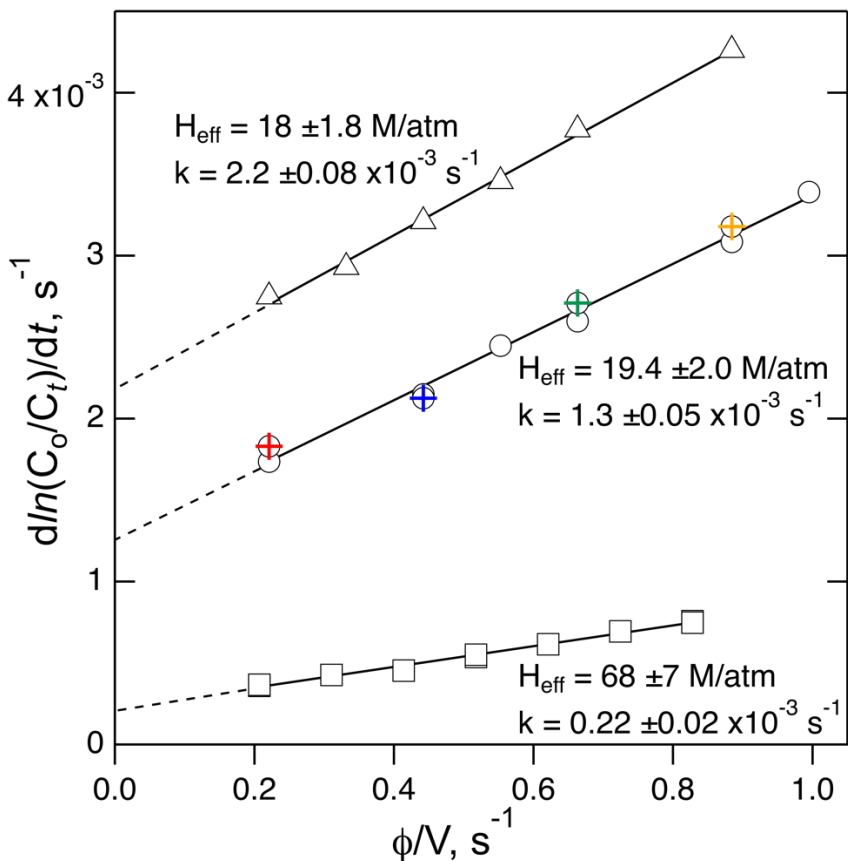


Figure S6. Summary of the decay rate data from Figures S3, S4, and S5, versus ϕ/V , and the associated H and k calculated from the fits. The errors in individual rate measurements are smaller than the width of the symbols.

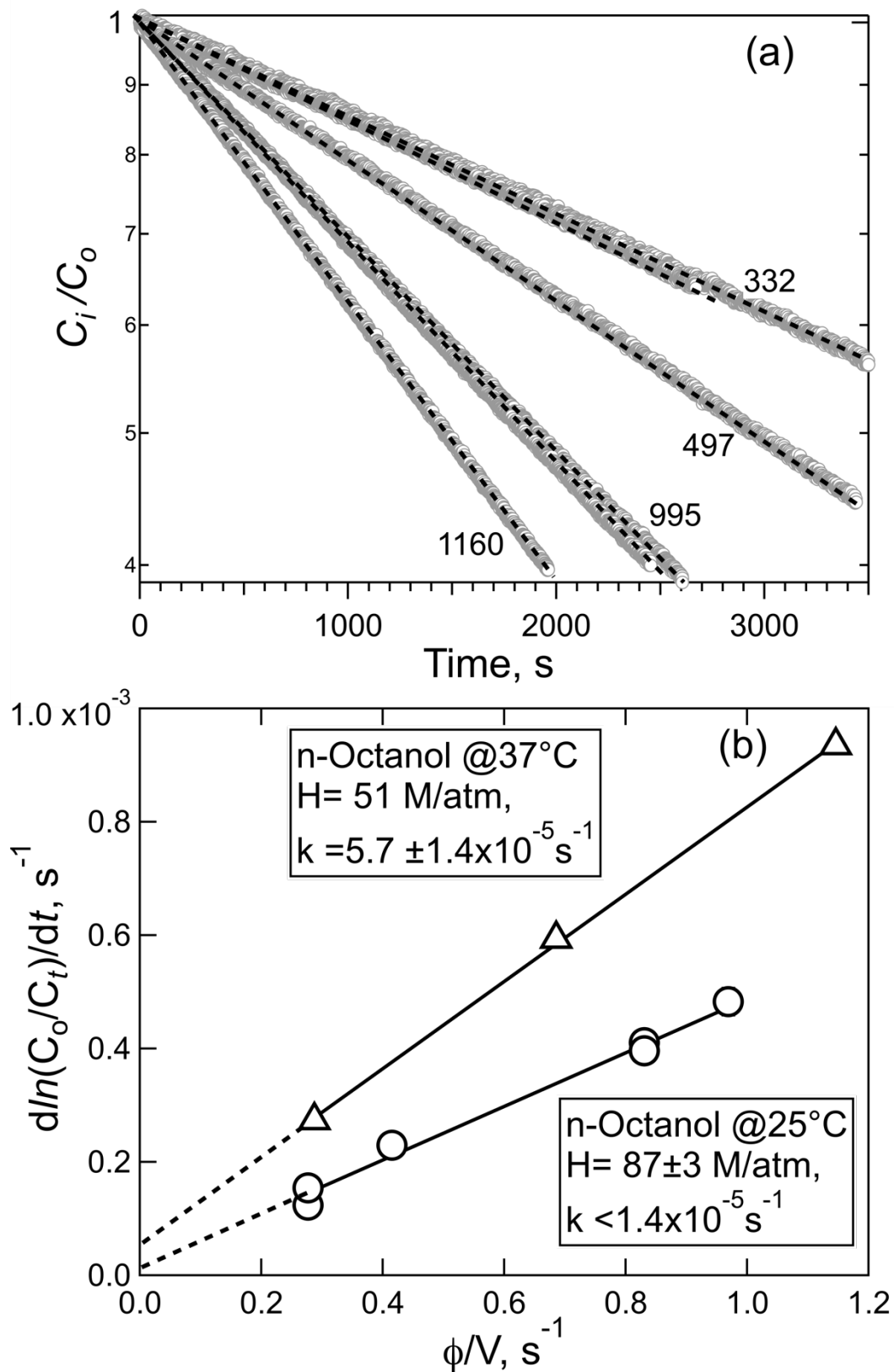


Figure S7. (a) The decay plots for the experiment with HNC0 in 20cc n-octanol at 298K. The dashed lines are exponential fits and the numbers shown are the flow rates in amb cc/min. (b) The summary of decay rates versus ϕ/V for both 298K (circles) and 310K (triangles). The errors in the individual decay rate determinations are smaller than the width of the symbols.

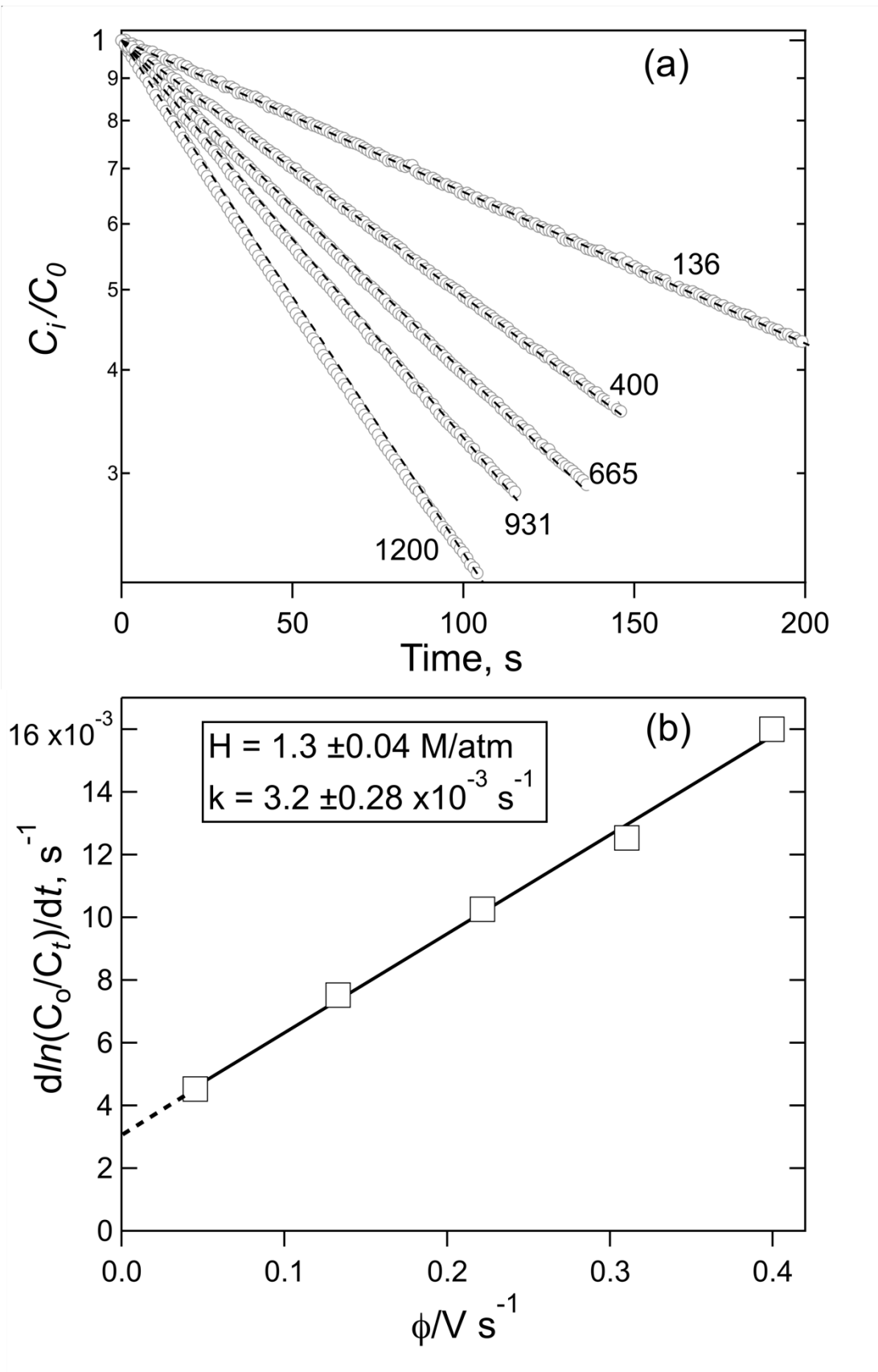


Figure S8. (a) The decay plots for the experiment with CH_3NCO in 50cc H_2O at pH2 and 298K. The dashed lines are exponential fits and the numbers shown are the flow rates in amb cc/min. (b) The summary of decay rates versus ϕ/V for the data in panel (a). The errors in the individual decay rate determinations are smaller than the width of the symbols.

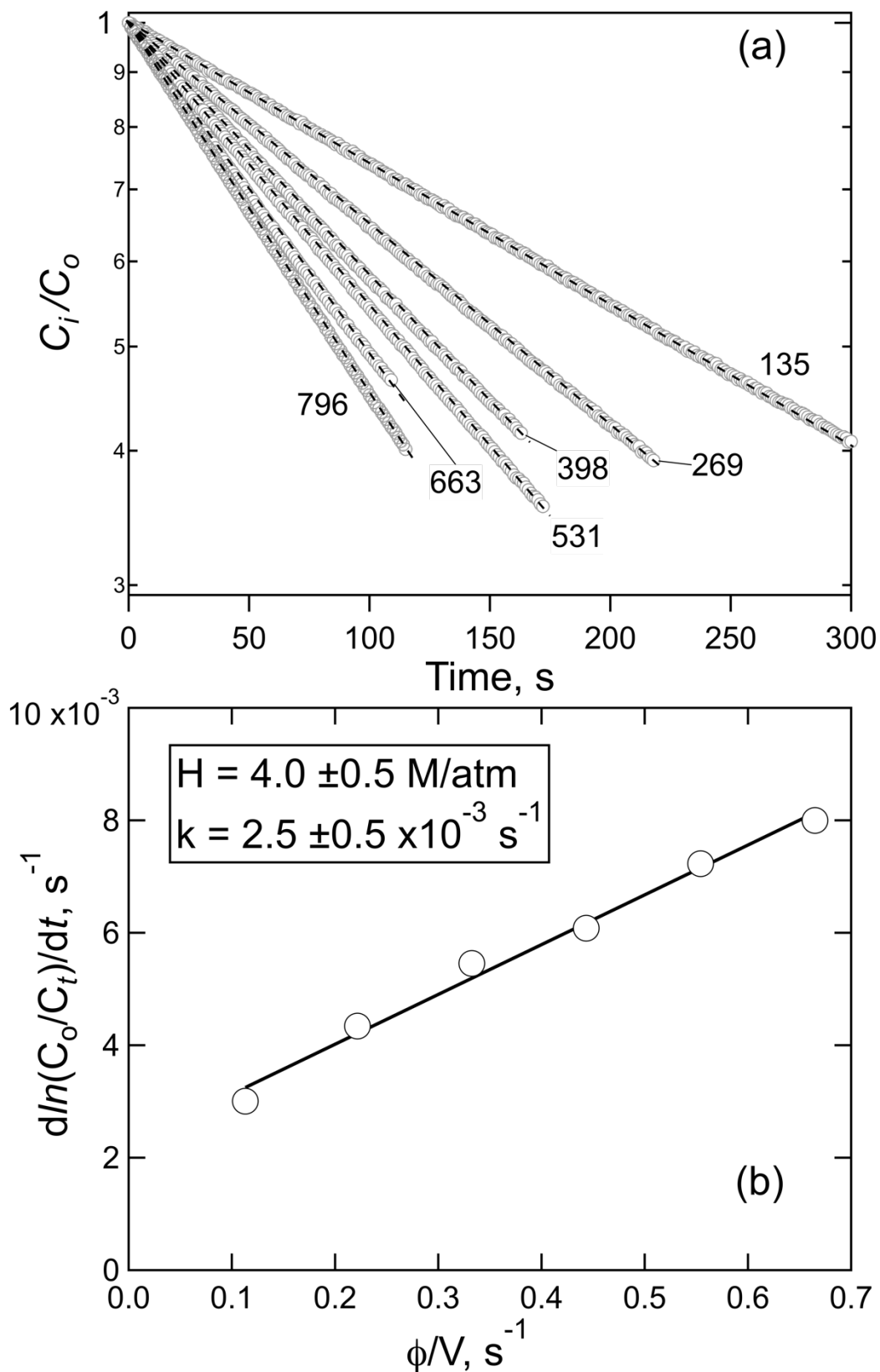


Figure S9. (a) The decay plots for the solubility experiment involving CH_3NCO in 20 cc of n-octanol at 298K. The dashed lines are exponential fits and the numbers shown are the flow rates in amb cc/min. (b) The plot of the CH_3NCO loss rates versus ϕ/V under the range of flow rates used. The errors in the individual decay rate determinations are smaller than the width of the symbols.

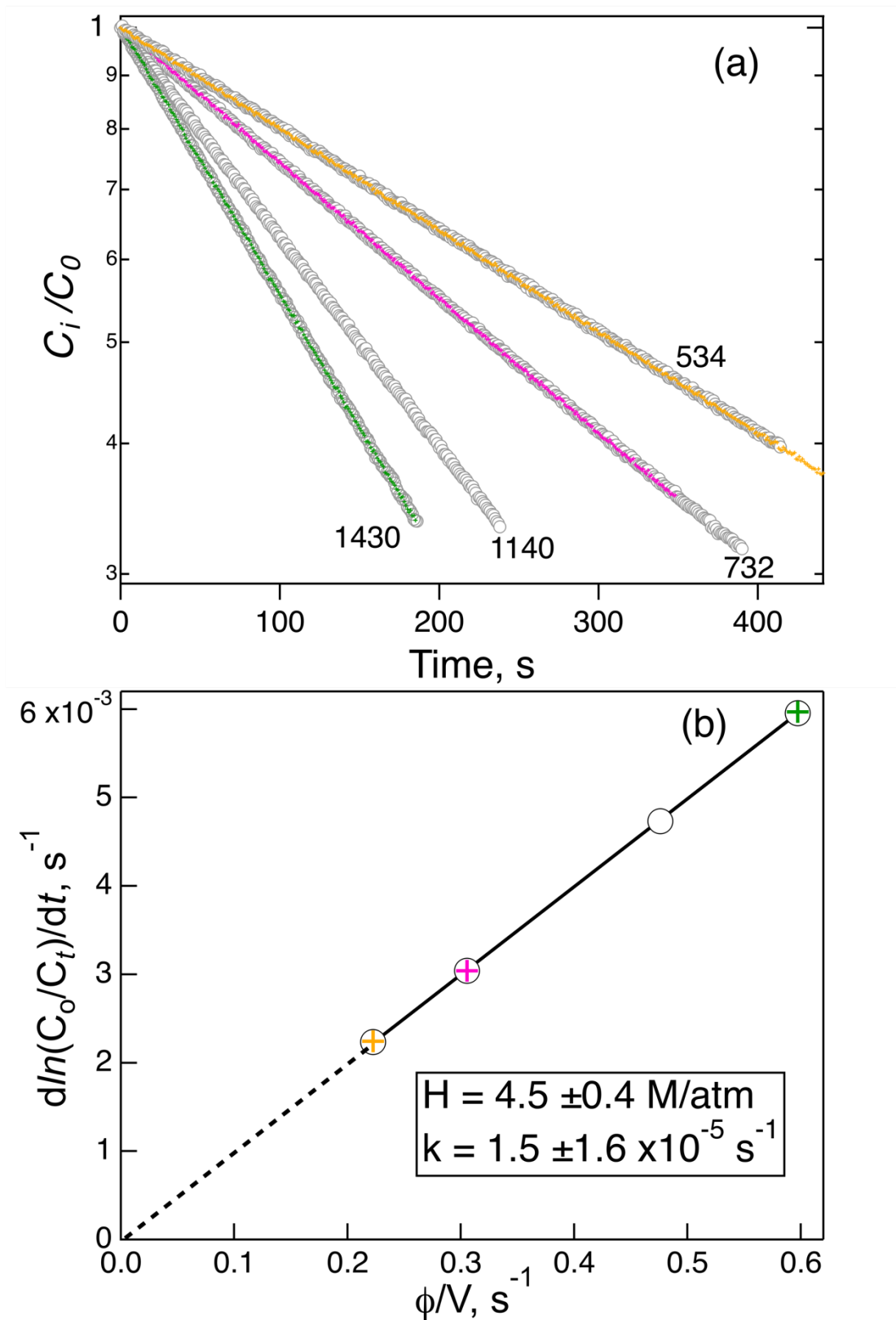


Figure S10. (a) The decay plots for the solubility experiment involving C1CN in 40 cc of H₂O at 273.15K. The numbers shown are the flow rates in amb cc/min, and duplicate runs are shown in colors. (b) The plot of the C1CN loss rates versus ϕ/V under the range of flow rates used. The errors in the individual decay rate determinations are smaller than the width of the symbols.

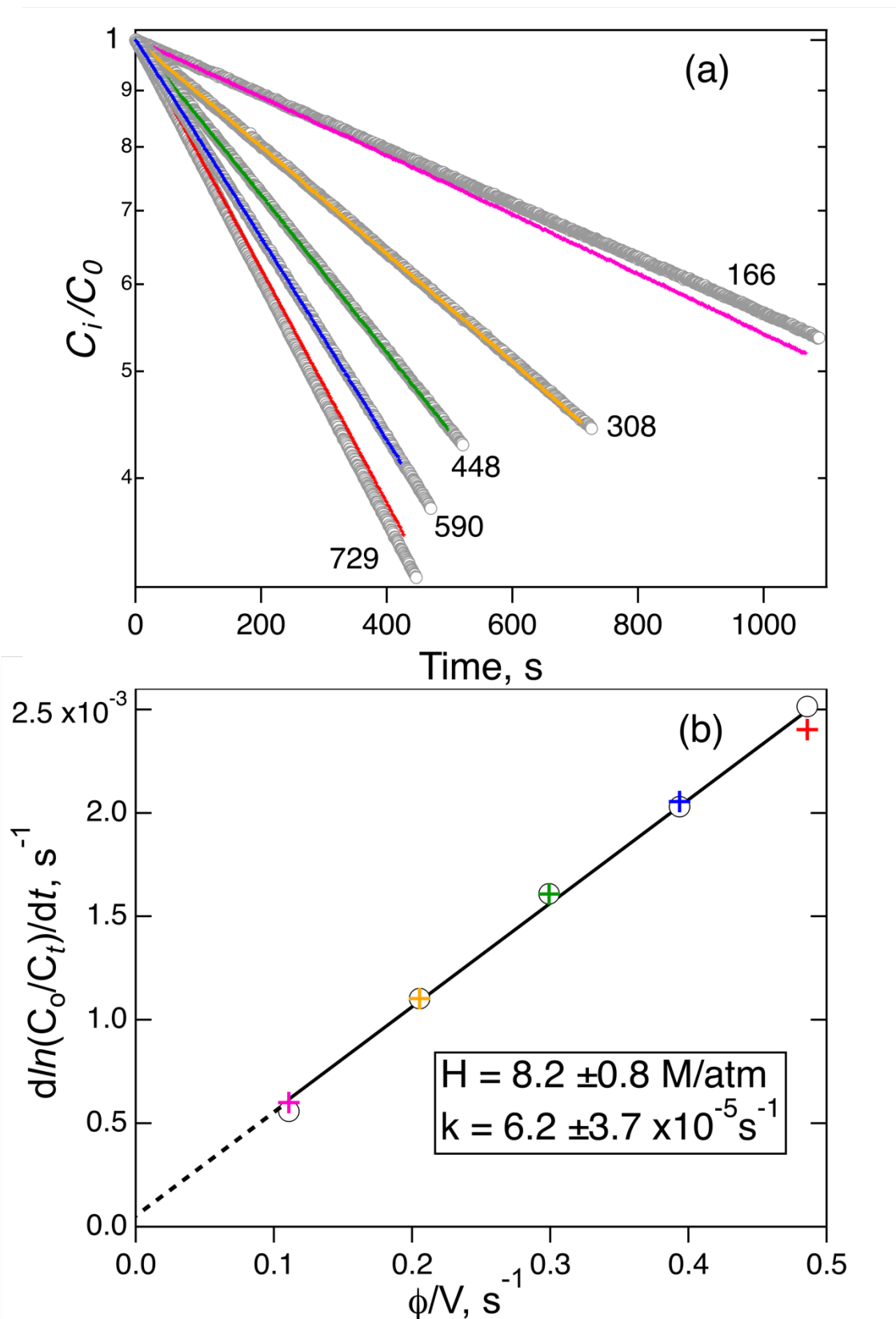


Figure S11. (a) The decay plots for the solubility experiment involving BrCN in 25 cc of H₂O at 296K. The numbers shown are the flow rates in amb cc/min, and duplicate runs are shown in colors. (b) The plot of the BrCN loss rates versus ϕ/V under the range of flow rates used. The errors in the individual decay rate determinations are smaller than the width of the symbols.

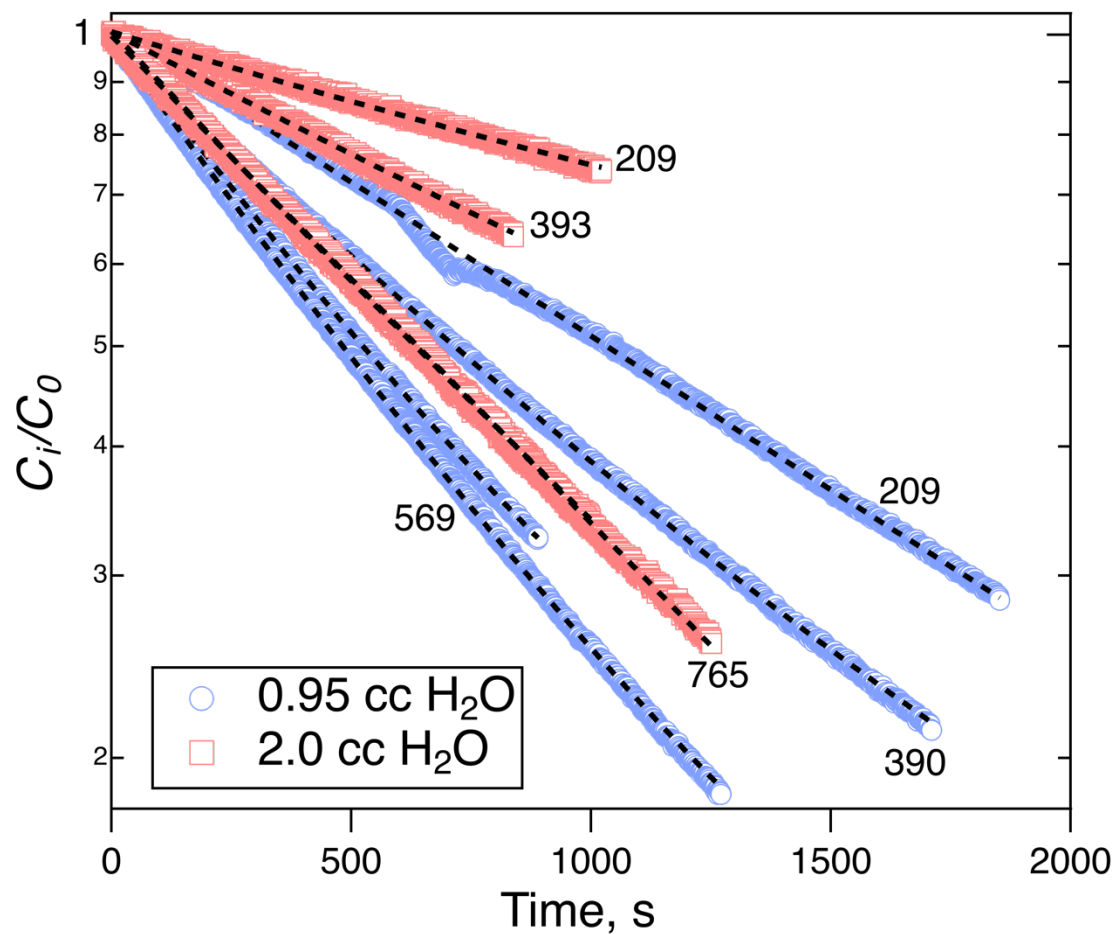


Figure S12. The decay plots for the solubility experiments shown in Figure 7 of the main paper involving ICN in 0.95 and 2.0 cc of H₂O at 298K. The dashed lines are exponential fits and the numbers shown are the flow rates in amb cc/min.

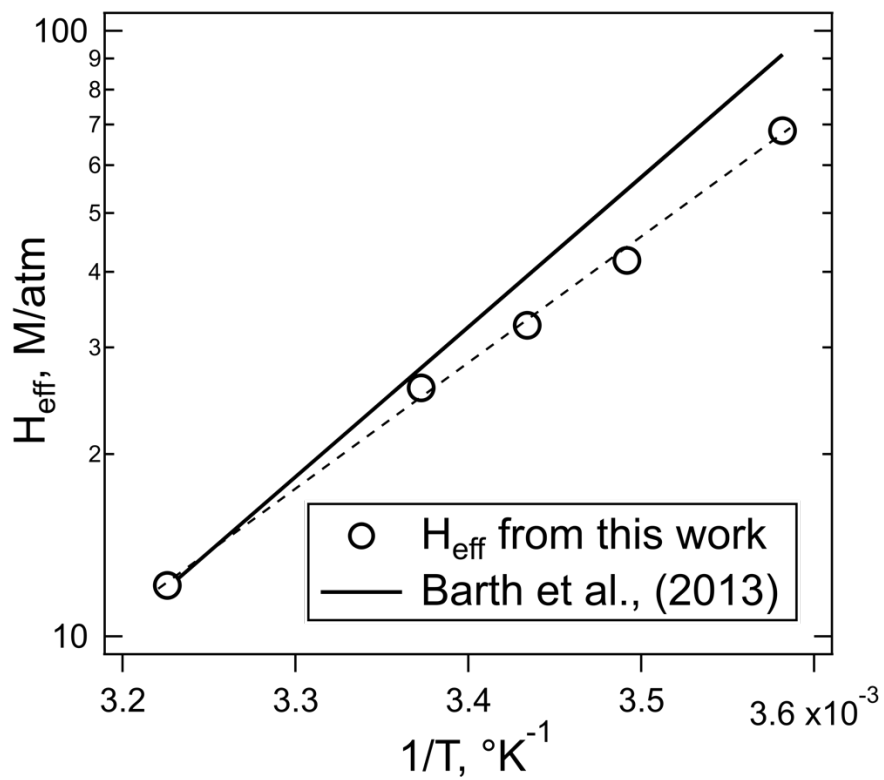


Figure S13. Comparison of the temperature dependence of H_{eff} for HNCO at pH3 between this work (circles and dashed line) with that used by the model of Barth et al., (2013) (solid line), which was based on the assumption that it was the same as for HC(O)OH.

Unlike HNCO and CH₃NCO, some of the XCN compounds have absorbances in the near UV-vis that could lead to photolysis in the lower atmosphere, Figure S14. The UV-vis spectra and photon fluxes estimated from the NCAR TUV model (NCAR, 2018) can be used to calculate photolysis rates, by integrating over the wavelength region where the absorption is significant, and assuming a quantum yield of 1. The absorption spectra are such that ClCN will not be photolyzed in the troposphere, BrCN has some slight absorption in the actinic region and ICN has substantial absorption. The lifetimes against photolysis at 0km altitude, 40°N, on June 30, 2015, were estimated to be 135 days for BrCN, and 9 hours for ICN.

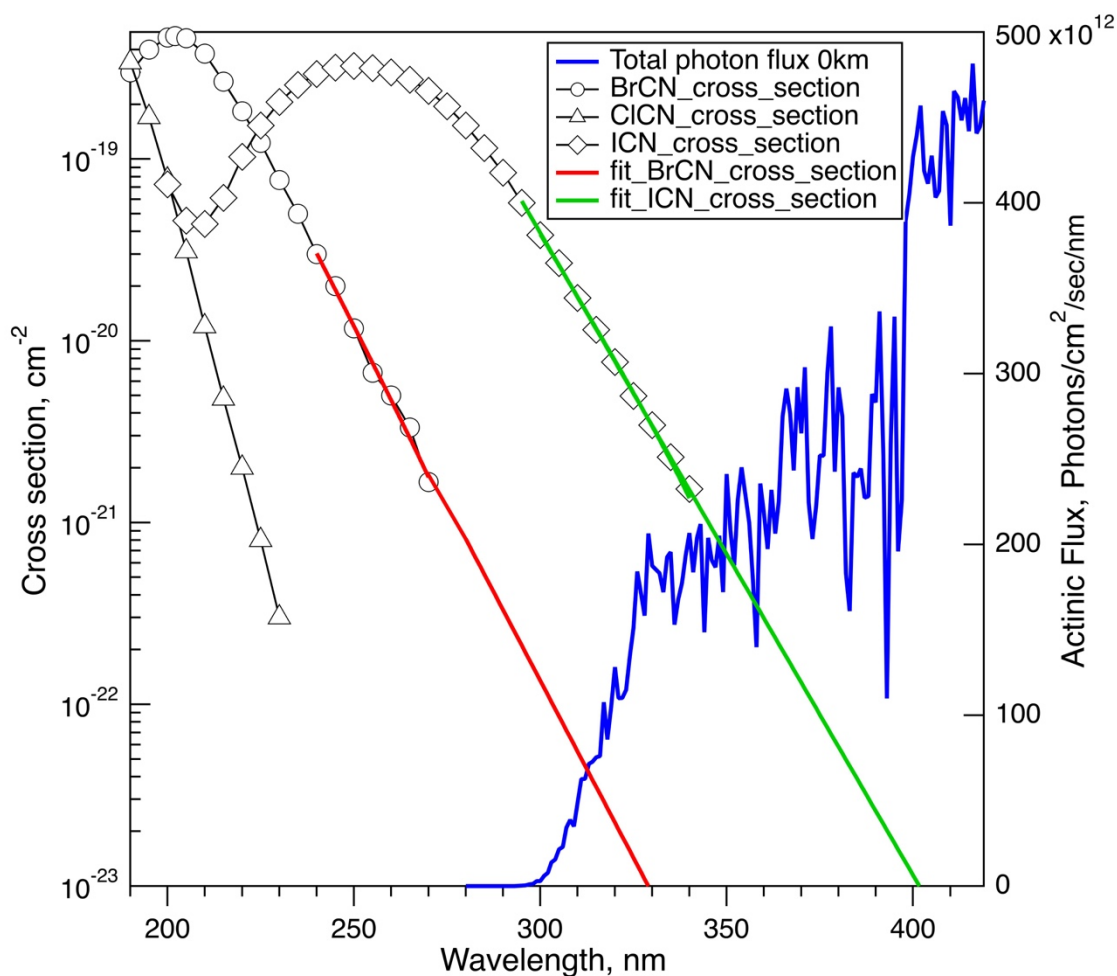


Figure S14. The UV-vis absorption spectra of ClCN, BrCN, ICN, (Barts and Halpern, 1989; Felps et al., 1991; Hess and Leone, 1987; Russell et al., 1987) and the photon flux spectrum estimated from the NCAR TUV model for 40° N, surface on June 30, 2015 (NCAR, 2018). The extrapolation assumes the cross-sections are ln-linear over the portions that tail into the actinic region.

References:

Barts, S. A. and Halpern, J. B.: Photodissociation of ClCN between 190 and 213 nm, J. Phys. Chem., 93, 7346-7351, 1989.

Felps, W. S., Rupnik, K., and McGlynn, S. P.: Electronic spectroscopy of the cyanogen halides. , J. Phys. Chem., 95, 639-656, 1991.

Hess, W. P. and Leone, S. R.: Absolute I* quantum yields for the ICN \tilde{A} state by diode laser gain-vs-absorption spectroscopy, J. Chem. Phys., 86, 3773-3780, 1987.

NCAR: http://cprm.acom.ucar.edu/Models/TUV/Interactive_TUV/, last access: September 1, 2018 2018.

Russell, J. A., McLaren, I. A., Jackson, W. M., and Halpern, J. B.: Photolysis of BrCN between 193 and 266 nm, J. Phys. Chem., 91, 3248-3253, 1987.